

Self-organization of Tactile Receptive Fields: Exploring Their Textural Origin and Their Representational Properties

Choonseog Park, Heeyoul Choi, and Yoonsuck Choe

Department of Computer Science and Engineering
Texas A&M University
College Station, TX 77843-3112
{cspark13,hchoi}@cs.tamu.edu,choe@tamu.edu

Abstract. In our earlier work, we found that feature space induced by tactile receptive fields (TRFs) are better than that by visual receptive fields (VRFs) in texture boundary detection tasks. This suggests that TRFs could be intimately associated with texture-like input. In this paper, we investigate how TRFs can develop in a cortical learning context. Our main hypothesis is that TRFs can be self-organized using the same cortical development mechanism found in the visual cortex, simply by exposing it to texture-like inputs (as opposed to natural-scene-like inputs). To test our hypothesis, we used the LISSOM model of visual cortical development. Our main results show that texture-like inputs lead to the self-organization of TRFs while natural-scene-like inputs lead to VRFs. These results suggest that TRFs can better represent texture than VRFs. We further analyzed the effectiveness of TRFs in representing texture, using kernel Fisher discriminant (KFD) and the results, along with texture classification performance, confirm that this is indeed the case. We expect these results to help us better understand the nature of texture, as a fundamentally tactile property.

1 Introduction

Humans process sensory information from different specialized modalities (e.g., vision, touch, and hearing), yet relatively little is known about how specific input stimuli affect the cortical organization. Textural patterns have been studied as important cues that help form the sensory cortex [1]. In our earlier work, tactile representation was found to be better than vision-based ones in texture tasks [2]. Given computational models based on visual receptive fields (VRFs) [3] and tactile receptive fields (TRFs) (Fig. 1) [4], those based on TRFs showed a significantly superior texture boundary detection performance compared to those based on VRFs (t-test: $n = 100, p < 0.03$) [2]. This suggests that TRFs are intimately related with texture-like input, and that texture is fundamentally tactile.

In this paper, we investigate how TRFs can self-organize and if texture-like input play a key role. Our main hypothesis is that TRFs can be self-organized

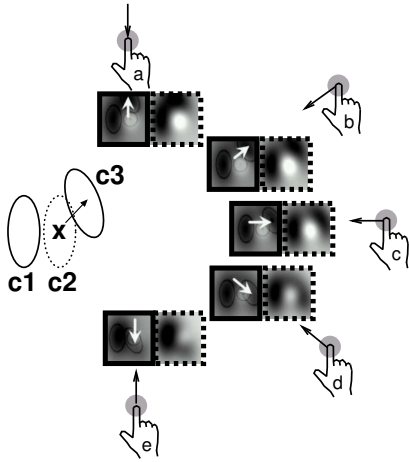


Fig. 1. Tactile Receptive Fields (TRFs). TRFs found in the somatosensory area 3b are similar to visual receptive fields (VRFs) (marked C1 and C2, representing inhibitory and excitatory blobs) but there is an added dynamic inhibitory component (marked C3). C3’s position relative to the fixed components change, centered at “X”, depending on the direction of scan of the tactile surface, e.g., the finger tip (right). The arrow on the finger tip shows the scan direction; the solid outline box shows how the dynamic inhibitory component is shifted (white arrow) in the opposite direction of the scan; and the dotted outline box shows the resulting TRF shape. Adapted from [5] (also see [4]).

using the a visual cortical development model by simply exposing it to texture-like inputs. In order to test our hypothesis, we used the LISSOM (Laterally Interconnected Synergetically Self-Organizing Map) model which was originally developed to model the self-organization of the visual cortex [6]. However, the LISSOM model is actually a more general model of how the cortex (in general) organizes to represent correlations in the sensory input, regardless of the input modality. Thus, LISSOM should work equally well in modeling the development of non-visual sensory modalities (e.g., see [7]).

Our main results show that texture-like inputs lead to the self-organization of TRFs while natural-scene-like inputs lead to VRFs. This result proposes that TRFs could have become accommodated to (surface) textures with a regular repetition of pattern, while VRFs adjusted to handle natural scenes containing various objects and backgrounds that do not repeat over space. We further analyzed the effectiveness of the TRFs and VRFs in representing texture, using kernel Fisher discriminant analysis (KFD) [8]. The results confirmed that TRFs are better suited for textures than VRFs.

The rest of this paper is organized as follows. Section 2 describes the process and results of self-organization using LISSOM. In section 3, a manifold analysis (KFD) for the TRF and VRF feature space is given. Section 4 discusses issues arising from our work, followed by the conclusion in section 5.

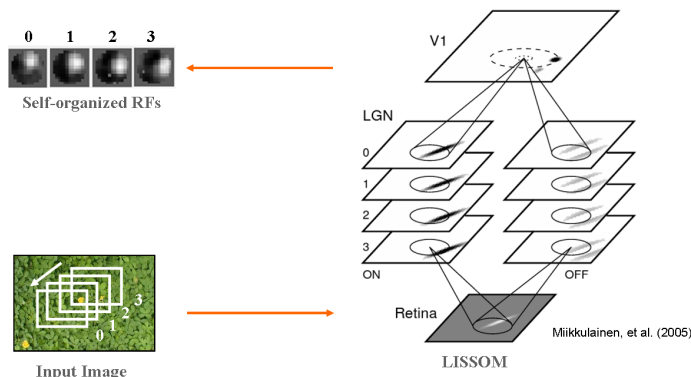


Fig. 2. Self-organization process with LISSOM. Given a large image, motion of the gaze window results in a sequence of inputs being generated on the LISSOM retina, which in turn activates the lateral geniculate nucleus (LGN) ON/OFF sheets, one by one, depending on the sheet’s built-in delay. After projecting the activities from the LGN ON/OFF sheets, V1 (the primary visual cortex) self-organizes its RFs and lateral connections (excitatory and inhibitory). LISSOM figure adapted from [6].

2 Self-organization of the tactile receptive fields

In order to investigate the developmental origin of TRFs, we used the Topographica neural map simulator package (<http://topographica.org>) [9, 6]. Topographica implements a superset of the LISSOM model.

Fig. 2 shows the experimental process we followed to develop self-organized RFs. We generated input stimulus that are natural-scene-like or texture-like, while sampling across the input image with the retina. Fig. 3 shows the inputs we used: natural-scenes and textures.

Given an image, we randomly picked an initial location and moved the gaze window in a random direction along a straight line at a fixed interval. Moving input on an image following a scanning direction are presented on the retina in discrete time steps, like frames of a movie. At each time step t , all LGN cells calculate their activities with lag t one after another as a scalar product of a fixed weight vector (standard on-center/off-surround and vice versa) and input response on the retinal sheet. Each V1 neuron computes its initial response like that of an LGN cell. After the initial response, the V1 activity settles through short-range excitatory and long-range inhibitory lateral interaction. Note that for the texture input, the above process simulates the somatosensory pathway, starting with the texture image standing in for raw mechanoreceptor activation array. After the activity has settled, the connection weights of each V1 neuron are modified according to the normalized Hebbian learning rule. The weakest connections are eliminated periodically, resulting in self-organized patterns similar to those observed in the cerebral cortex. See [6] for details.

For the simulation reported in this paper, four 24×24 LGN-ON cell sheets and four 24×24 LGN-OFF cell sheets received input from a 48×48 retinal sheet,



Fig. 3. Sample Input Patterns. The top row shows natural scenes and the bottom row textures used in our experiments. Note that the texture set has texture elements at varying scales. Adapted from [5].

and a 48×48 V1 sheet was used to self-organize the RFs. The learning parameters were the same as in the basic LISSOM model in Topographica [6] with small modification of several scaling factors for low-contrast inputs of images as described in the appendices of [6].

Fig. 4 shows the self-organized RFs of six representative V1 neurons trained with texture-like input and natural-scene-like input after 20,000 training iterations. The self-organized RFs produced from LISSOM with the texture input set are visualized in Fig. 4a. The neurons developed spatiotemporal RFs strongly resembling tactile RFs found in the somatosensory cortex (Fig. 1) [4]: excitatory (bright) and inhibitory (dark) components of each neuron consists of ring and blob-like features. Note that these RF shapes arise not because circular texture elements dominate the texture input set we used. There are interesting variations as well, such as the last three columns in Fig. 4a. In those RFs, the polarity is reversed, i.e., instead of an excitatory region in the middle and inhibitory region in the surround, these RFs have an inhibitory region in the middle and the excitatory region in the surround.

On the other hand, RFs self-organized based on natural-scene-like inputs show a significantly different pattern. Nearly all neurons in Fig. 4b developed spatiotemporal RFs strongly selective for both direction and orientation. The receptive fields consist of excitatory (bright) and inhibitory (dark) lobes according to the preferred orientation and direction of the neuron, showing spatiotemporal preference. That is, each neuron is highly responsive to a line with a particular orientation moving in a direction perpendicular to that orientation. Such properties of the receptive fields are similar to those of the receptive fields of neurons found experimentally in the visual cortex [10].

The overall layout (i.e., map organization) of the RFs developed in these simulations is shown in Fig. 5 (roughly every 3rd neuron is plotted, horizontally and vertically). The texture input set we used show texture elements at varying scales, however, on closer observation, the size of the receptive field (15×15) is usually smaller than the round or oval features in the texture input set. So, these receptive fields are not direct memorization of the dominant features in the

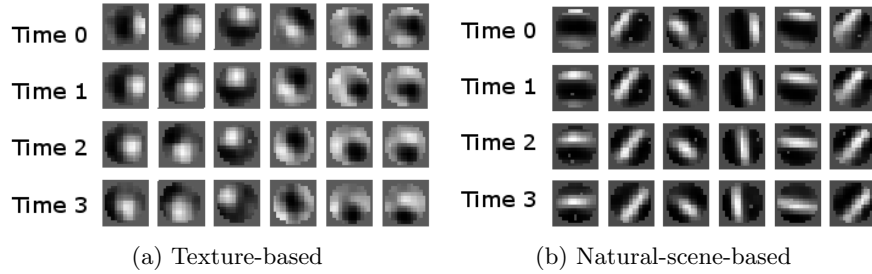


Fig. 4. RFs Resulting from Self-Organization on the Natural Scene Input Set. Six spatiotemporal RFs from (a) the texture (b) the natural-scene based experiments are shown. Each column corresponds to an individual neuron’s RF, and each column represents the different time-lag. In (a), the RF shapes resemble the ring-like shape of tactile RFs found in [4] (also see Fig. 1). In (b) we can see that the pattern moves in a direction perpendicular to the orientation preference as in [10]. Adapted from [5].

texture input set. Note that Fig. 5 only shows the first frame among the total of four (note that these are spatiotemporal RFs). Fig. 5b shows the map trained with natural inputs, and here we can see most RFs have a oriented Gabor-like property, just like in the visual cortex [6]. Fig. 6 shows the orientation selectivity histograms for the two maps: texture-based and natural-scene-based. The natural-scene based map (i.e., the “visual” map) shows a much higher orientation selectivity.

The results show that exposure to texture-like input can drive a general cortical learning model to develop RFs that resemble tactile RFs, while exposure to natural-scene-like input leads to visual RFs. The significance of this results is that it shows an intimate connection between texture and the tactile modality.

3 Manifold analysis of RF response

The responses of the RFs are represented in high-dimensional feature spaces, and it is hard to interpret. An effective approach for analyzing the characteristics of the responses is to assume that the responses of each RF lie on a non-linear low-dimensional manifold embedded in the high dimensional feature space. Each embedded manifold is spanned by a few dominant factors. In order to find the dominant factors of the features, we applied kernel Fisher discriminant (KFD) [11] to the feature spaces of the RF response. Here, we briefly review KFD.

KFD is a generalized version of Fisher discriminant analysis (or linear discriminant analysis, LDA) using kernel trick as in support vector machines or kernel principal component analysis [12]. The basis function in the feature space can be obtained by maximizing the ratio of the within-class scatter matrix in the feature space to the between-class scatter matrix in the feature space, as in LDA. Let $\mathcal{X}_i = \{x_1^i, x_2^i, \dots, x_{i_i}^i\}$, ($i = 1, \dots, C$), be samples from C classes and

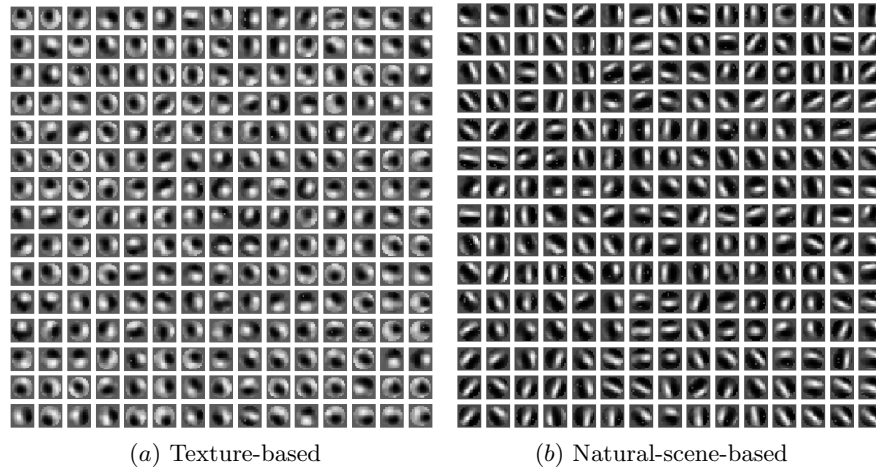


Fig. 5. RFs Resulting from Self-Organization on (a) the Texture Input Set and (b) the Natural-Scene Input Set. From the 48×48 cortex, only 15×15 are plotted (roughly every 3rd RF) for a detailed view of the RFs. The RFs in (a) mostly resemble tactile RFs while the RFs in (b) mostly resemble visual RFs. Adapted from [5].

$\mathcal{X} = \bigcup_i^C \mathcal{X}_i$. Suppose $\Phi(\cdot)$ is a nonlinear mapping function to the feature space, then the within-class scatter matrix in feature space, \mathbf{S}_W^Φ , is given by

$$\mathbf{S}_W^\Phi = \sum_{i=1}^C \sum_{x \in \mathcal{X}_i} (\Phi(x) - m_i^\Phi)(\Phi(x) - m_i^\Phi)^T, \quad (1)$$

where $m_i^\Phi = \frac{1}{l_i} \sum_{j=1}^{l_i} \Phi(x_j^i)$. The between-class scatter matrix in feature space is given by $\mathbf{S}_B^\Phi = \mathbf{S}_T^\Phi - \mathbf{S}_W^\Phi$, where the total scatter matrix in feature space, \mathbf{S}_T^Φ , is given by

$$\mathbf{S}_T^\Phi = \sum_{x \in \mathcal{X}} (\Phi(x) - m^\Phi)(\Phi(x) - m^\Phi)^T, \quad (2)$$

where $m^\Phi = \frac{1}{|\mathcal{X}|} \sum_{i=1}^C l_i m_i^\Phi$ and $|\mathcal{X}|$ is the sample size.

We applied KFD to the responses of TRF and VRF on texture-like inputs (three textures were from Fig. 3). Fig. 7 shows the two different embedded manifold (TRF-based and VRF-based) in two-dimensional space. We used the square root function as the kernel function for both cases. The figure shows that the TRF responses give clusters that are more separable across texture classes than those based on VRF responses.

In order to further quantify the merit of the different RF types in dealing with texture, we measured the classification performance on the KFD results. We ran the experiment for 30 times and for each experiment 50% of data set was

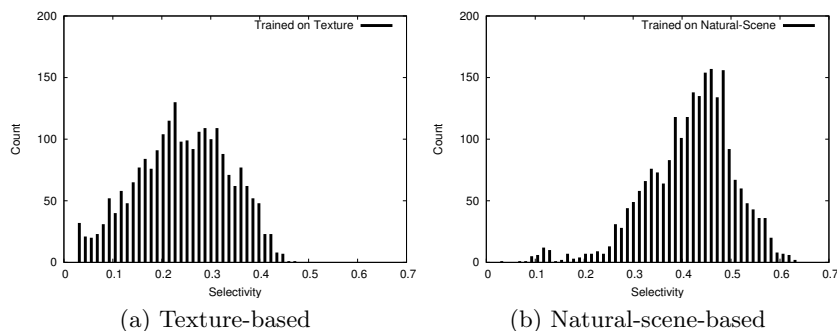


Fig. 6. Selectivity in Orientation Maps. The orientation selectivity histogram are shown for the two 48×48 V1 sheets (maps): (a) texture-based map, and (b) natural-scene-based map. As we can already see from Fig. 5, the map trained with natural scenes show much higher selectivity (peak near 0.45), compared to the case with textures (peak near 0.25). Note that higher selectivity means that RFs are more sharply tuned to one specific orientation (i.e., RFs are more slender).

randomly chosen as training data and the rest as testing data. As a classifier, k-nearest neighbor (kNN) was used. Fig. 8 shows the boxplot of the classification rate for both RFs on texture-like inputs. The averages were 89.8% (for TRF-based) and 83.4% (for VRF-based), respectively. We can see that TRF is better than VRF in texture classification task. Another interesting thing is that the standard deviation in the TRF case ($= 0.0121$) is less than that of the VRF case ($= 0.0156$), which means that the performance of the TRF-based representation is more stable than that of the VRF. We also conducted a similar experiment, this time on natural-scene inputs, but the results were inconclusive, i.e., both TRFs and VRFs showed an equal level of (high) performance in the scene classification task. We are currently investigating the cause, since we expected VRFs to be better than TRFs for this task.

4 Discussion and Conclusion

The main contribution of this work is to have shown a developmental and a functional relationship between tactile RFs and texture. We have shown that texture-like input can drive the self-organization of tactile RFs, and tactile RFs are more effective in dealing with texture than visual RFs. The novelty of our result is not that it showed changed RF organization due to altered stimulus statistics, since that is already well-established (see [6] for a review). The novelty of our work is more specific, by explicitly linking texture to tactile RF development. The results in this paper further confirm our initial insight on the nature of texture: texture as a surface property in 3D [13]. From a computational perspective, it is also interesting to note that the TRF response distribution shows a power-law property, which is known to indicate sparse representations (see [5] for the data). Sparse coding is known to provide an efficient representation for

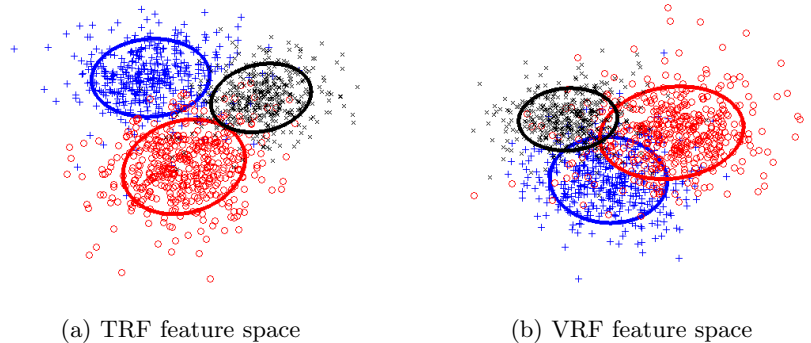


Fig. 7. Kernel Fisher discriminant (KFD) feature spaces for TRF and VRF responses. KFD analysis of (a) TRF and (b) VRF responses to texture-like input are shown. In each plot, response samples from three different textures, projected on the 1st and 2nd KFD axes, are shown. The ellipses show the $1.5 \times \sigma$ equidistance trace from the class centers. We can see that the classes in (a) are more separable than those in (b).

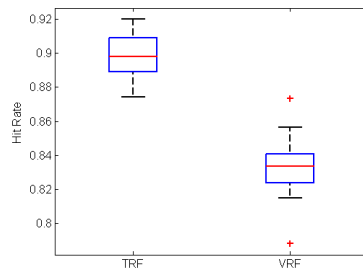


Fig. 8. Comparison of texture classification rate based on TRF response (left) and VRF response (right) to texture-like input is shown. The box plot shows the quartile, median, and the upper quartile, while the whiskers show 1.5 times the interquartile range (“+” marks outliers, $n = 30$). TRF-based response shows higher texture classification performance.

natural scenes and receptive field characteristics, similar to those found in the primary visual cortex [14]. Finally, it would be interesting to apply our finding in the investigation of visuo-tactile integration in the blind. The use of texture as the stimulus can help tease out the common functional processes in the two different modalities (cf. [15]).

To conclude, the main objective of this work was to confirm the relationship between tactile RFs and texture. The results suggest that tactile RFs can be self-organized by texture-like input using a general cortical development model (LISSOM) initially inspired by the visual cortex, and that the representations from tactile RFs are better than vision-based ones for texture tasks. We expect our results to help us better understand the nature of texture, as a fundamentally tactile property.

Acknowledgments: Part of the results in section 2 (Figs. 4&5) has been accepted for presentation in [5]. This research was funded in part by NIH/NIMH (#1R01-MH66991) and NIH/NINDS (#1R01-NS54252).

References

1. Knierim, J.J., van Essen, D.C.: Neuronal responses to static texture pattern in area v1 of the alert macaque monkey. *Neurophysiol.* **67** (1992) 961–980
2. Bai, Y.H., Park, C., Choe, Y.: Relative advantage of touch over vision in the exploration of texture. In: Proceedings of the 19th International Conference on Pattern Recognition, Tampa, FL. (2008) In press.
3. Jones, J.P., Palmer, L.A.: An evaluation of the two-dimensional Gabor filter model of simple receptive fields in cat striate cortex. *Neurophysiology* **58**(6) (1987) 1233–1258
4. DiCarlo, J.J., Johnson, K.O.: Spatial and temporal structure of receptive fields in primate somatosensory area 3b: Effects of stimulus scanning direction and orientation. *Neuroscience* **20** (March 2000) 495–510
5. Park, C., Bai, Y.H., Choe, Y.: Tactile or visual?: Stimulus characteristics determine RF type in a self-organizing map model of cortical development. In: Proceedings of 2009 IEEE Symposium on Computational Intelligence for Multimedia Signal and Vision Processing, Nashville, TN. (2009) To appear.
6. Miikkulainen, R., Bednar, J.A., Choe, Y., Sirosh, J.: *Computational Maps in the Visual Cortex*. Springer, New York, NY (2005)
7. Wilson, S.: Self-organisation can explain the mapping of angular whisker deflections in the barrel cortex. Master’s thesis, The University of Edinburgh, Scotland, United Kingdom (2007)
8. Khurd, P., Baloch, S., Gur, R., Davatzikos, C., Verma, R.: Manifold learning techniques in image analysis of high-dimensional diffusion tensor magnetic resonance images. In: the IEEE Conference on CVPR. (2007)
9. Bednar, J.A., Choe, Y., De Paula, J., Miikkulainen, R., Provost, J., Tversky, T.: Modeling cortical maps with Topographica. *Neurocomputing* (2004) 1129–1135
10. DeAngelis, G.C., Ghose, G.M., Ohzawa, I., Freeman, R.D.: Functional micro-organization of primary visual cortex: Receptive-field analysis of nearby neurons. *Neuroscience* **19** (1999) 4046–4064
11. Mika, S., Ratsch, G., Weston, J., Schölkopf, B., Müller, K.: Fisher discriminant analysis with kernels. In: Proceedings of IEEE Neural Networks for Signal Processing Workshop. (1999) 41–48
12. Schölkopf, B., Smola, A.J.: *Learning with Kernels*. MIT Press (2002)
13. Oh, S., Choe, Y.: Segmentation of textures defined on flat vs. layered surfaces using neural networks: Comparison of 2D vs. 3D representations. *Neurocomputing* **70** (2007) 2245–2255
14. Olshausen, B.A., Field, D.J.: Emergence of simple-cell receptive field properties by learning a sparse code for natural images. *Nature* **381** (1996) 607–609
15. Grant, A.C., Thiagarajah, M.C., Sathian, K.: Tactile perception in blind braille readers : A psychophysical study of acuity and hyperacuity using gratings and dot patterns. *Perception and Psychophysics* **62** (2000) 301–312